

New perspectives on shocks, cosmic rays, and magnetic fields in galaxy clusters

Christoph Pfrommer^{1,2}

in collaboration with

L. Jonathan Dursi¹, Anders Pinzke³, Torsten EnBlin⁴, Volker Springel⁴

¹Canadian Institute for Theoretical Astrophysics, Canada

²Heidelberg Institute for Theoretical Studies, Germany

³Stockholm University, Sweden

⁴Max-Planck Institute for Astrophysics, Germany

24 Aug 2010 / Physics of the Intracluster Medium, Michigan



Outline

- 1 **Magnetic draping on spiral galaxies**
 - Polarized radio ridges
 - Physics of magnetic draping
 - Implications and speculations
- 2 **Cosmic rays in clusters**
 - Physical processes
 - Cosmological simulations
 - Gamma-ray emission
- 3 **Conclusions**



Outline

- 1 Magnetic draping on spiral galaxies**
 - Polarized radio ridges
 - Physics of magnetic draping
 - Implications and speculations
- 2 Cosmic rays in clusters
 - Physical processes
 - Cosmological simulations
 - Gamma-ray emission
- 3 Conclusions

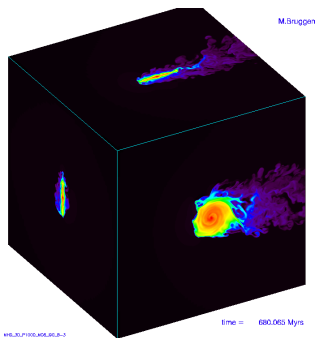
Polarized synchrotron emission in a field spiral: M51



MPIfR Bonn and Hubble Heritage Team

- polarized synchrotron intensity follows the spiral pattern and is strongest in between the spiral arms (NGC 6946)
- the polarization 'B-vectors' are aligned with the spiral structure
- a promising generating mechanism is the *dynamo which transfers mechanical into magnetic energy* (Beck et al. 1996)

Ram-pressure stripping of cluster spirals

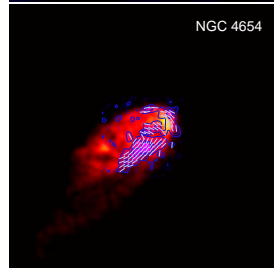
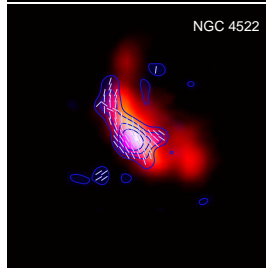
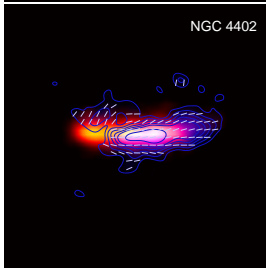
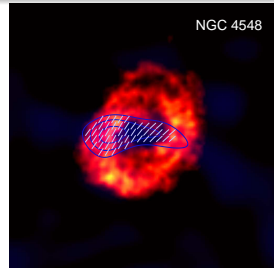
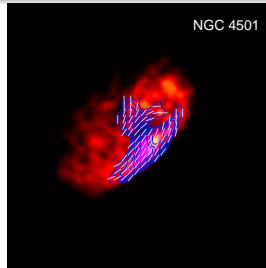
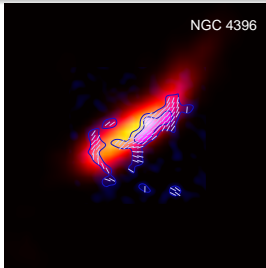


Brueggen (2008)

- 3D hydrodynamical simulations show that low-density gas in between spiral arms is quickly stripped irrespective of disk radius (Tonnesen & Bryan 2010)
- being flux-frozen into this dilute plasma, the large scale field will also be stripped, leaving behind the small scale field in the star forming regions

→ beam depolarization effects and superposition of causally unconnected star forming patches along the line-of-sight cause the **resulting radio synchrotron emission to be effectively unpolarized**

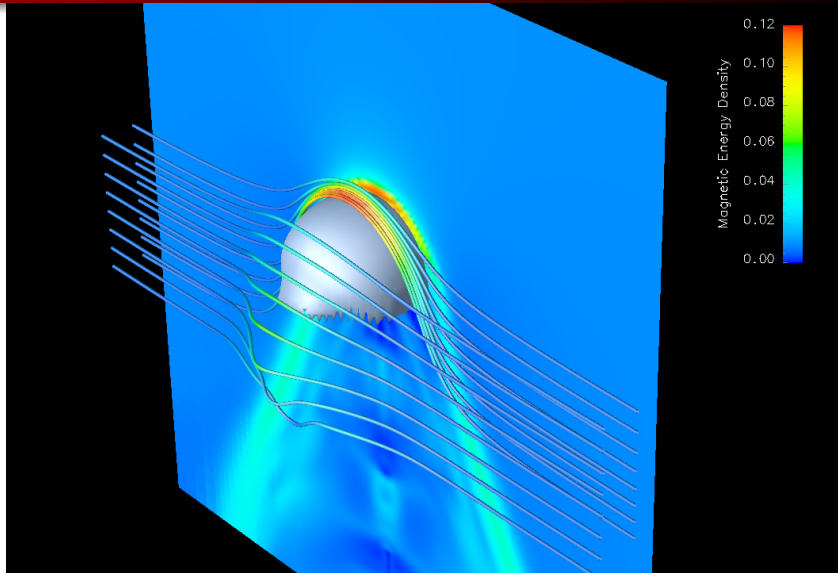
Polarized synchrotron ridges in Virgo spirals



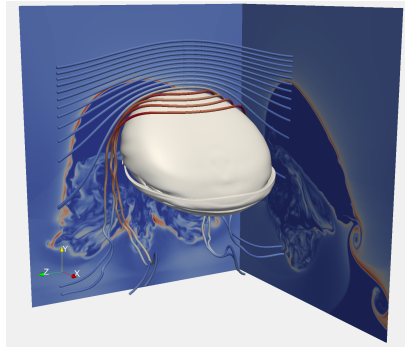
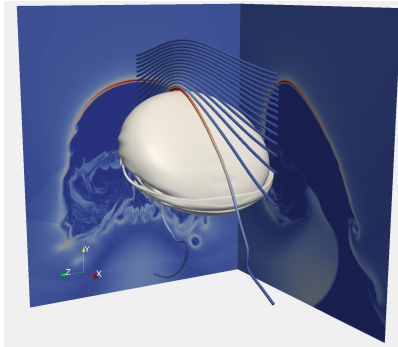
Vollmer et al. (2007): 6 cm PI (contours) + B-vectors; Chung et al. (2009): HI (red)



Draping field lines around a moving object

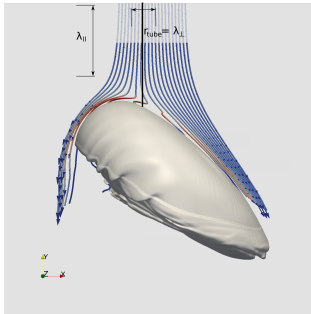


Magnetic draping around a spiral galaxy – MHD



Athena simulations of spiral galaxies interacting with a uniform cluster magnetic field. There is a **sheath of strong field draped around the leading edge** (field strength is color coded).

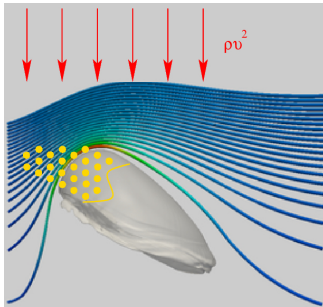
Streamlines in the rest frame of the galaxy



- as the flow approaches the galaxy it decelerates and gets deflected
- only those streamlines initially in a narrow tube of radius $\lambda_{\perp} \simeq R/\sqrt{3\beta\mathcal{M}^2} \simeq R/15 \simeq 1.3 \text{ kpc}$ from the stagnation line become part of the magnetic draping layer (color coded) \rightarrow constraints on λ_B

- the streamlines that do not intersect the tube get deflected away from the galaxy, become never part of the drape and eventually get accelerated (Bernoulli effect)
- note the kink feature in some draping-layer field lines due to back reaction as the solution changes from the hydrodynamic potential flow solution to that in the draped layer

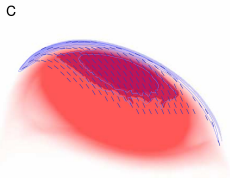
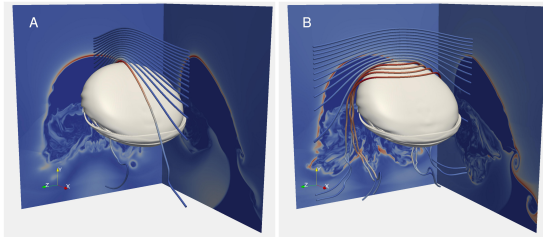
Magnetic draping around a spiral galaxy – physics



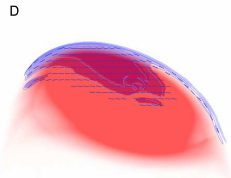
- the galactic ISM is pushed back by the ram pressure wind $\sim \rho v^2$
 - the stars are largely unaffected and lead the gas
 - the draping sheath is formed at the contact of ISM/ICM
 - as stars become SN, their remnants accelerate CRes that populate the field lines in the draping layer
-
- CRes are transported diffusively (along field lines) and advectively as field lines slip over the galaxy
 - CRes emit radio synchrotron radiation in the draped region, tracing out the field lines there → **coherent polarized emission at the galaxies' leading edges**

Magnetic draping and polarized synchrotron emission

Synchrotron B-vectors reflect the upstream orientation of cluster magnetic fields



Total PI = 8.227 mJy
Max PI = 218.7 μ Jy/beam



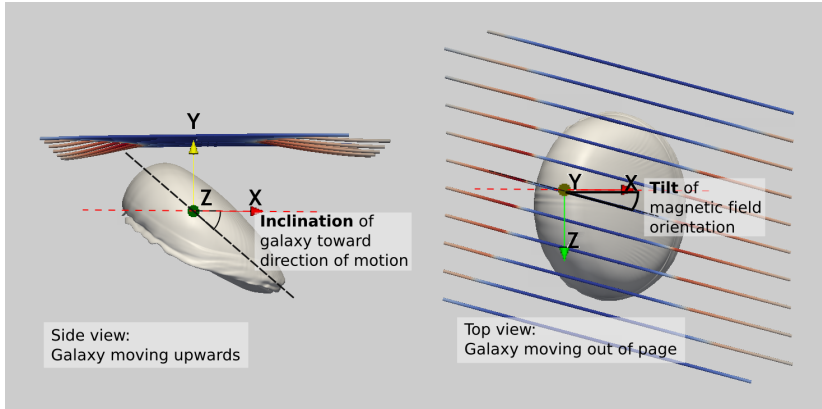
Total PI = 8.440 mJy
Max PI = 334.6 μ Jy/beam



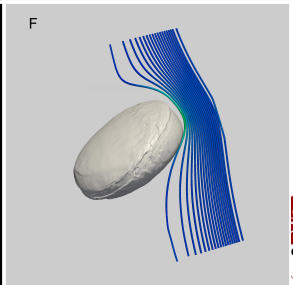
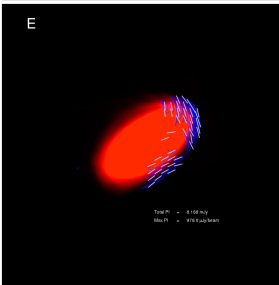
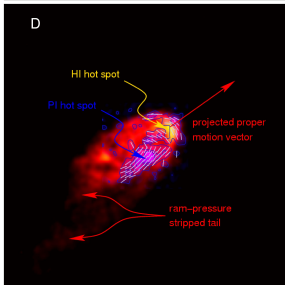
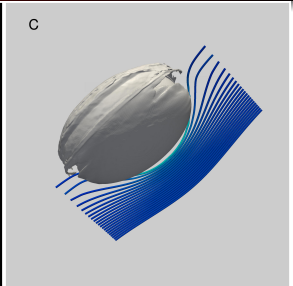
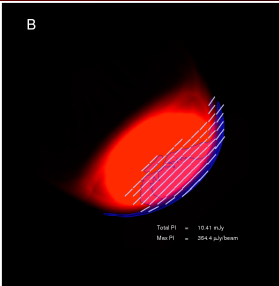
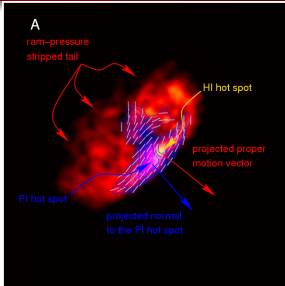
CITA-ICAT



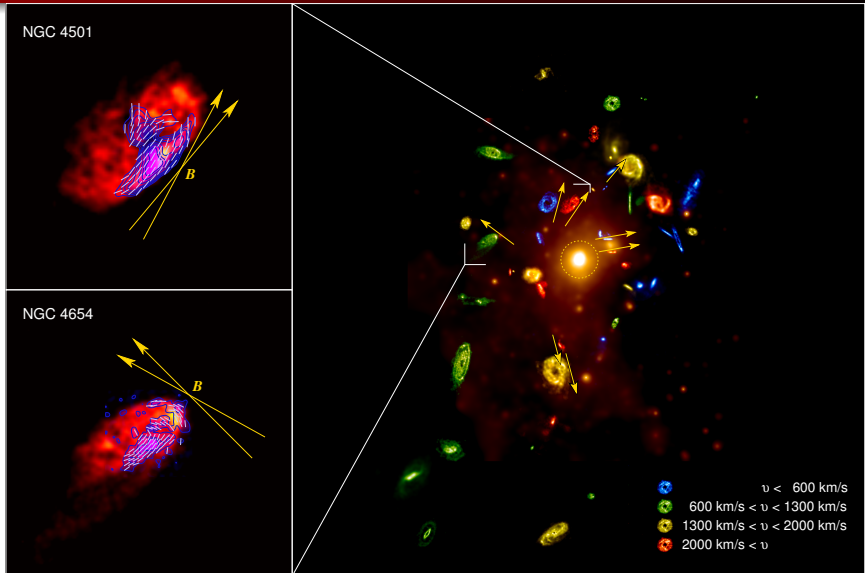
Varying galaxy inclination and magnetic tilt



Observations versus simulations



Mapping out the magnetic field in Virgo



Magneto-thermal instability: the idea

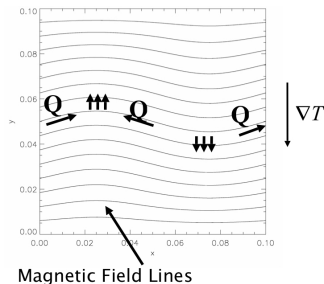


Figure from I. Parrish

Convective stability in a gravitational field:

- Classical Schwarzschild criterion:
 $\frac{dS}{dz} > 0$
- long MFP, Balbus criterion: $\frac{dT}{dz} > 0$
- **new instability causes field lines to reorient radially → efficient thermal conduction radially (close to Spitzer)**

The non-linear behavior of the MTI (Parrish & Stone 2007).

- **Adiabatic boundary conditions for $T(r)$** : the instability can exhaust the source of free energy → isothermal profile
- **Fixed boundary conditions for $T(r)$** : field lines stay preferentially radially aligned (35 deg mean deviation from radial)



Magneto-thermal instability: the idea

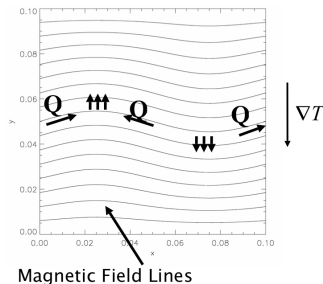


Figure from I. Parrish

Convective stability in a gravitational field:

- Classical Schwarzschild criterion:
 $\frac{dS}{dz} > 0$
- long MFP, Balbus criterion: $\frac{dT}{dz} > 0$
- **new instability causes field lines to reorient radially → efficient thermal conduction radially (close to Spitzer)**

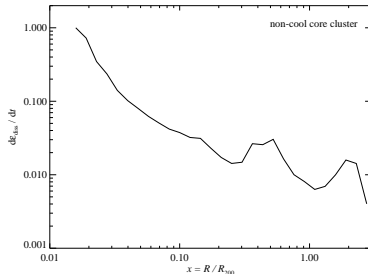
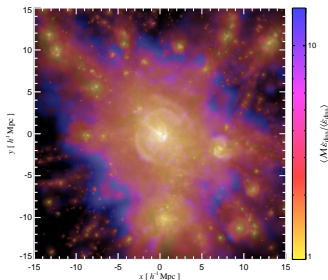
The non-linear behavior of the MTI (Parrish & Stone 2007).

- **Adiabatic boundary conditions for $T(r)$** : the instability can exhaust the source of free energy → isothermal profile
- **Fixed boundary conditions for $T(r)$** : field lines stay preferentially radially aligned (35 deg mean deviation from radial)



Gravitational shock wave heating

The **observed temperature profile in clusters is decreasing outwards** which is the necessary condition for MTI to operate \rightarrow *gravitational heating can stabilize the temperature profile:*

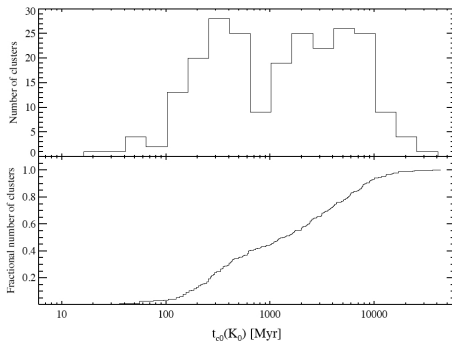


Mach number distribution weighted by ϵ_{diss} .

Energy flux through shock surface
 $\dot{E}_{\text{diss}} / R^2 \sim \rho v^3 \rightarrow$ increase towards the center



Implications for thermal stability of galaxy clusters



Cavagnolo et al. (2009)

- radial fields in non-cool core clusters (NCCs) imply efficient thermal conduction that **stabilizes these systems against entering a cool-core state**: $\tau_{cond} = \lambda^2 / \chi_C \simeq 2.3 \times 10^7 \text{ yr} (\lambda / 100 \text{ kpc})^2$, where χ_C is the Spitzer thermal diffusivity (using $kT = 10 \text{ keV}$, $n = 5 \times 10^{-3} \text{ cm}^{-3}$)
- current cosmological cluster simulations fail to reproduce NCCs that have no AGN activity \rightarrow **MHD + anisotropic conduction**



Magnetic draping at spiral galaxies in the Virgo cluster

nature
physics

ARTICLES

PUBLISHED ONLINE: 16 MAY 2010 | DOI: 10.1038/NPHYS1657

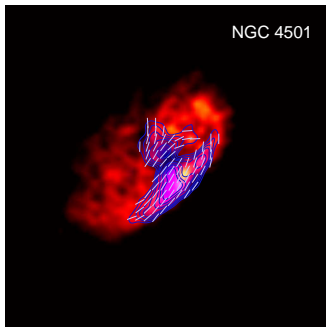
Detecting the orientation of magnetic fields in galaxy clusters

Christoph Pfrommer^{1*} and L. Jonathan Dursi^{1,2}

Clusters of galaxies, filled with hot magnetized plasma, are the largest bound objects in existence and an important touchstone in understanding the formation of structures in our Universe. In such clusters, thermal conduction follows field lines, so magnetic fields strongly shape the cluster's thermal history; that some have not since cooled and collapsed is a mystery. In a seemingly unrelated puzzle, recent observations of Virgo cluster spiral galaxies imply ridges of strong, coherent magnetic fields offset from their centre. Here we demonstrate, using three-dimensional magnetohydrodynamical simulations, that such ridges are easily explained by galaxies sweeping up field lines as they orbit inside the cluster. This magnetic drape is then lit up with cosmic rays from the galaxies' stars, generating coherent polarized emission at the galaxies' leading edges. This immediately presents a technique for probing local orientations and characteristic length scales of cluster magnetic fields. The first application of this technique, mapping the field of the Virgo cluster, gives a startling result: outside a central region, the magnetic field is preferentially oriented radially as predicted by the magnetothermal instability. Our results strongly suggest a mechanism for maintaining some clusters in a 'non-cooling-core' state.

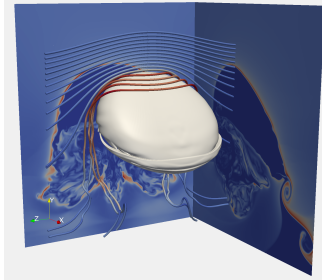


Conclusions on magnetic draping around galaxies



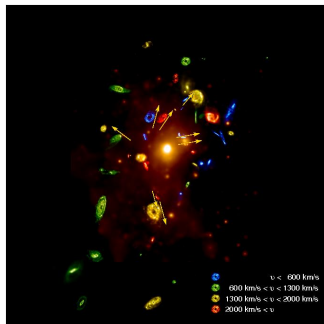
- draping of cluster magnetic fields naturally explains polarization ridges at Virgo spirals

Conclusions on magnetic draping around galaxies



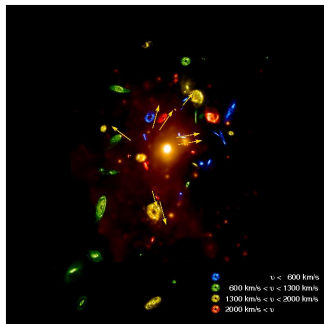
- draping of cluster magnetic fields naturally explains polarization ridges at Virgo spirals
- this represents a new tool for measuring the in situ orientation and coherence scale of cluster magnetic fields

Conclusions on magnetic draping around galaxies



- draping of cluster magnetic fields naturally explains polarization ridges at Virgo spirals
- this represents a new tool for measuring the in situ orientation and coherence scale of cluster magnetic fields
- application to the Virgo cluster shows that the magnetic field is preferentially aligned radially

Conclusions on magnetic draping around galaxies



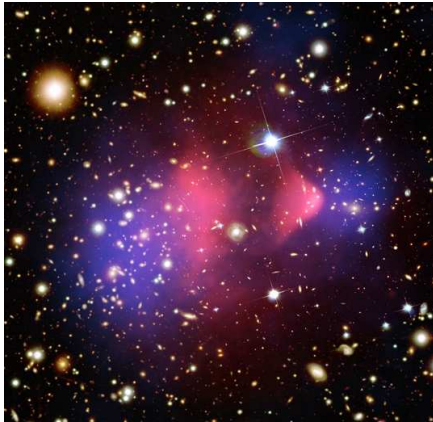
- draping of cluster magnetic fields naturally explains polarization ridges at Virgo spirals
 - this represents a new tool for measuring the in situ orientation and coherence scale of cluster magnetic fields
 - application to the Virgo cluster shows that the magnetic field is preferentially aligned radially
-
- this finding is suggestive that the MTI may be operating and implies efficient thermal conduction close to the Spitzer value
 - it also proposes that non-cool core clusters are stabilized by thermal conduction

Outline

- 1 Magnetic draping on spiral galaxies
 - Polarized radio ridges
 - Physics of magnetic draping
 - Implications and speculations
- 2 **Cosmic rays in clusters**
 - Physical processes
 - Cosmological simulations
 - Gamma-ray emission
- 3 Conclusions

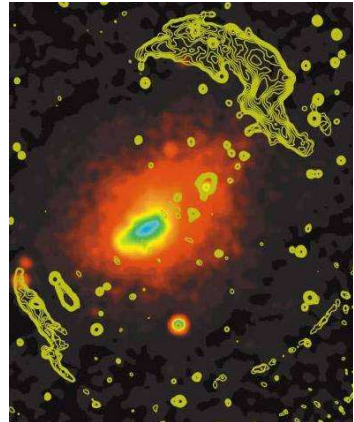


Shocks in galaxy clusters



1E 0657-56 (“Bullet cluster”)

(X-ray: NASA/CXC/CfA/M.Markevitch et al.; Optical: NASA/STScI; Magellan/U.Arizona/D.Clowe et al.; Lensing: NASA/STScI; ESO WFI; Magellan/U.Arizona/D.Clowe et al.)



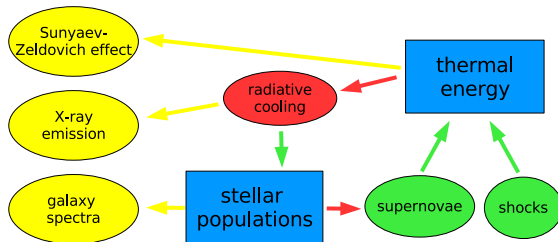
Abell 3667

(radio: Johnston-Hollitt. X-ray: ROSAT/PSPC.)

Radiative simulations with GADGET – flowchart

Cluster observables:

Physical processes in clusters:



CP, EnBlin, Springel (2008)

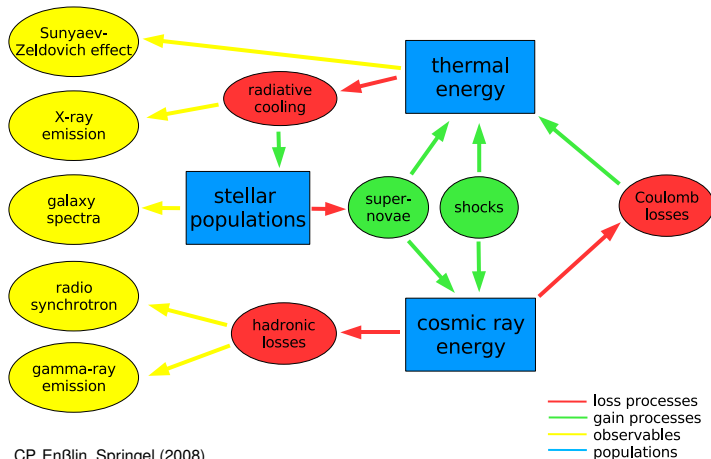
— loss processes
— gain processes
— observables
— populations



Radiative simulations with cosmic ray (CR) physics

Cluster observables:

Physical processes in clusters:

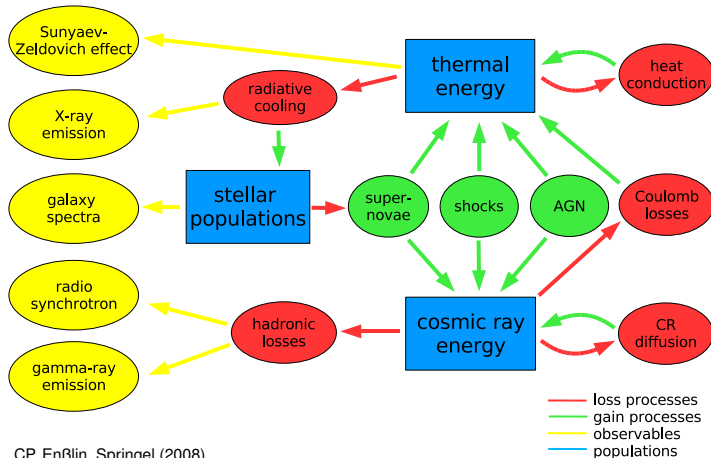


CP, EnBlin, Springel (2008)

Radiative simulations with extended CR physics

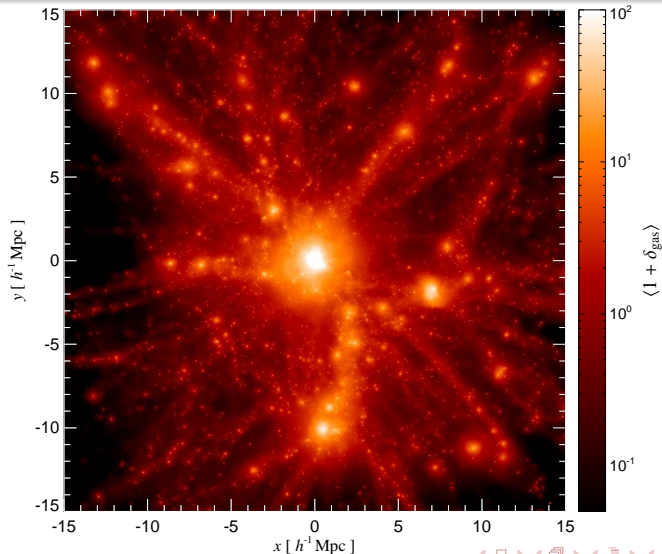
Cluster observables:

Physical processes in clusters:

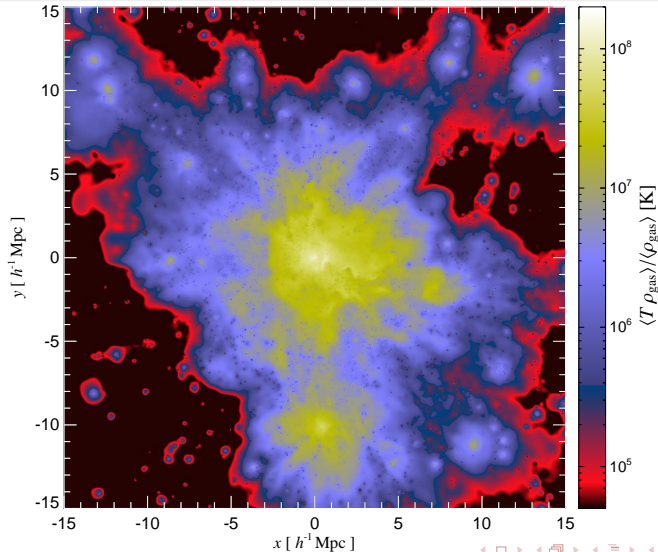


CP, EnBlin, Springel (2008)

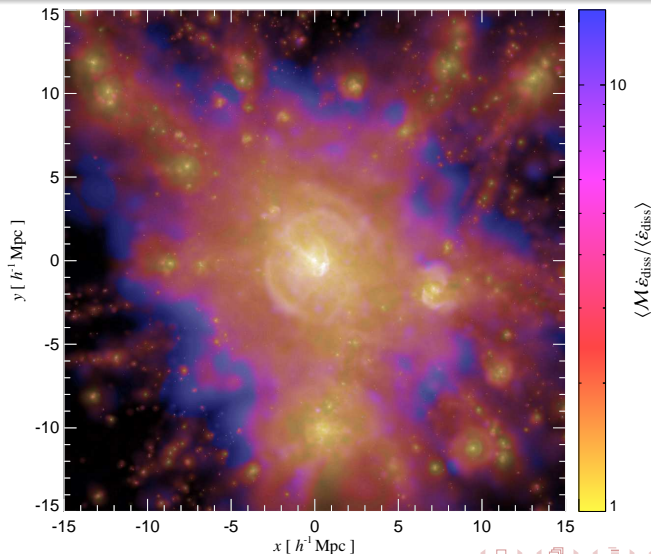
Radiative cool core cluster simulation: gas density



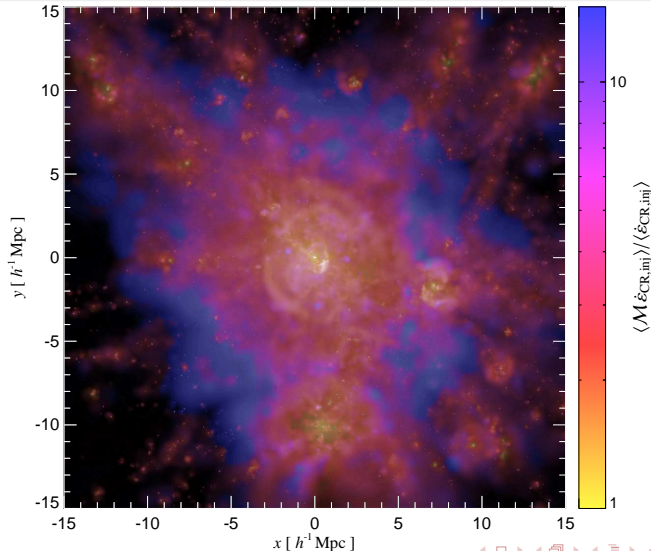
Mass weighted temperature



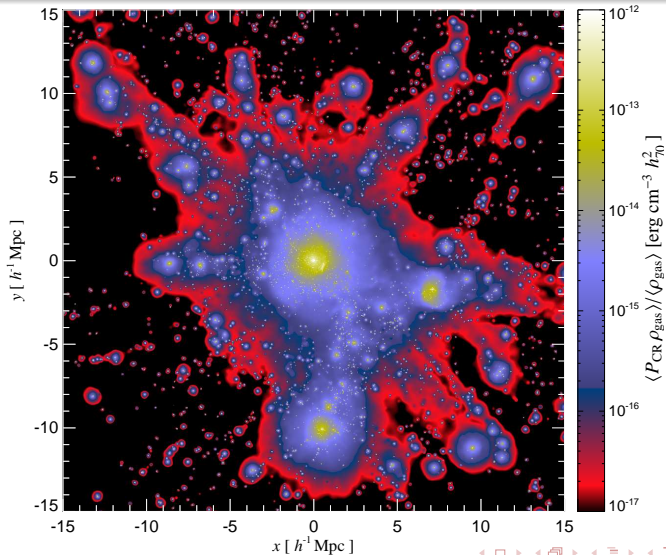
Mach number distribution weighted by ϵ_{diss}



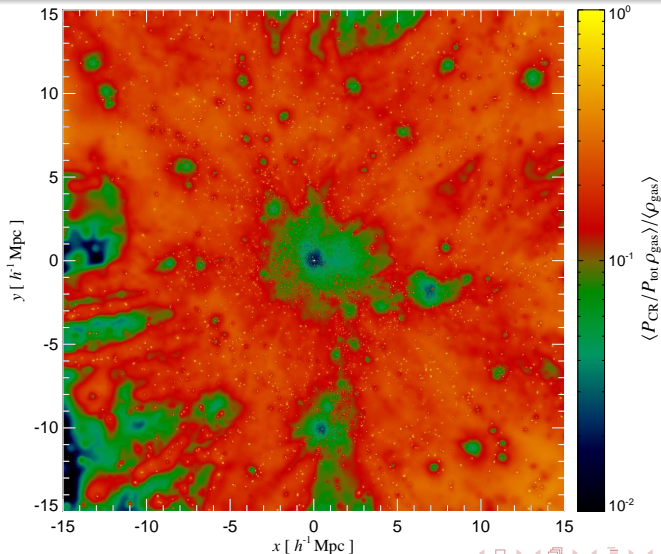
Mach number distribution weighted by $\varepsilon_{\text{CR},\text{inj}}$



CR pressure P_{CR}

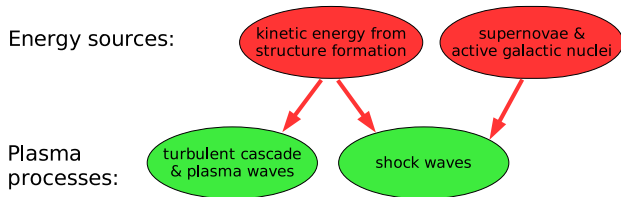


Relative CR pressure $P_{\text{CR}}/P_{\text{total}}$



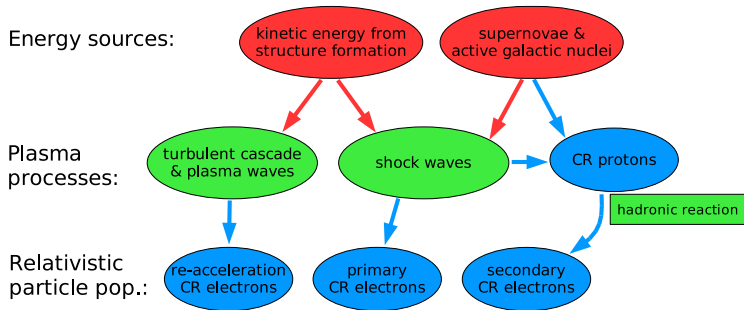
Multi messenger approach for non-thermal processes

Relativistic populations and radiative processes in clusters:



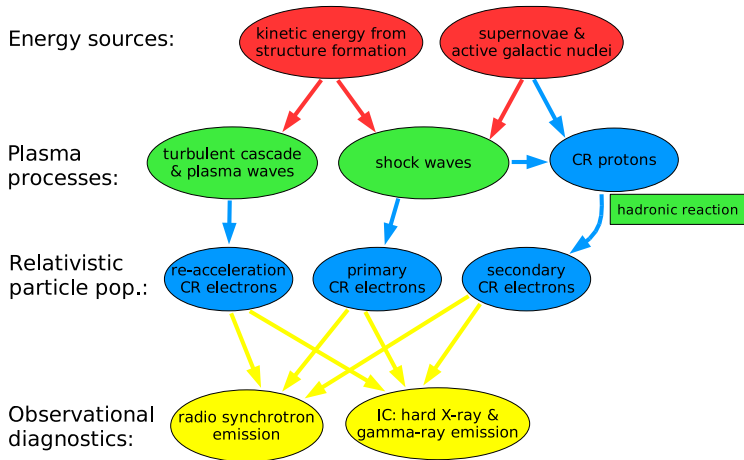
Multi messenger approach for non-thermal processes

Relativistic populations and radiative processes in clusters:



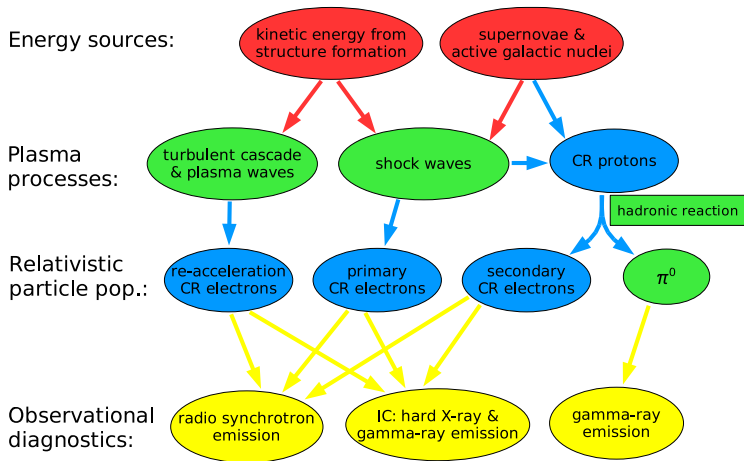
Multi messenger approach for non-thermal processes

Relativistic populations and radiative processes in clusters:

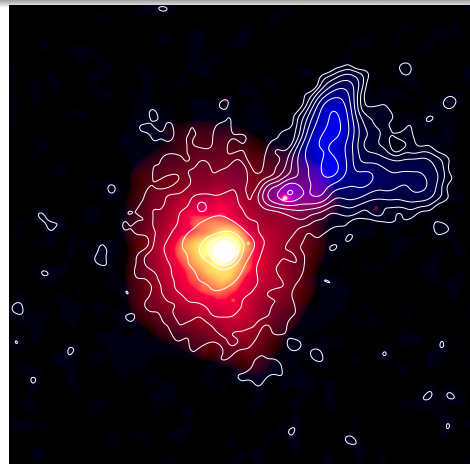
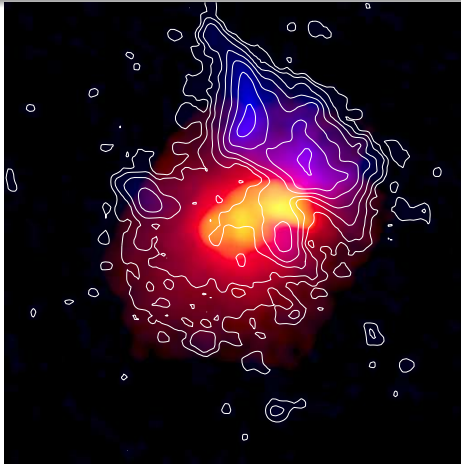


Multi messenger approach for non-thermal processes

Relativistic populations and radiative processes in clusters:

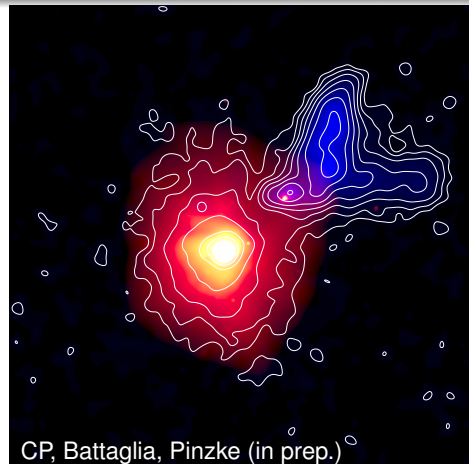
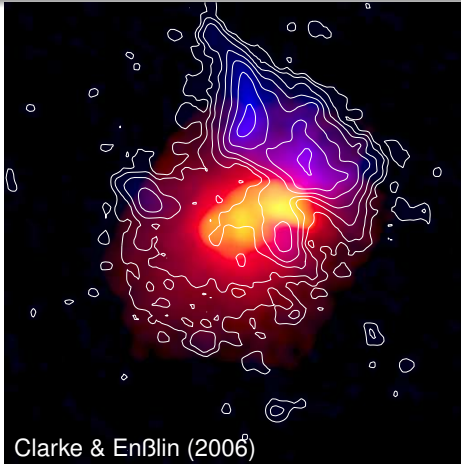


Which one is the simulation/observation of A2256?



red/yellow: thermal X-ray emission,
blue/contours: 1.4 GHz radio emission with giant radio halo and relic

Observation – simulation of A2256



red/yellow: thermal X-ray emission,
blue/contours: 1.4 GHz radio emission with giant radio halo and relic

Non-thermal emission from clusters

Exploring the memory of structure formation

- **primary, shock-accelerated CR electrons** resemble current accretion and merging shock waves
- **CR protons/hadronically produced CR electrons** trace the time integrated non-equilibrium activities of clusters that is modulated by the recent dynamical activities

How can we read out this information about non-thermal populations?

→ **new era of multi-frequency experiments**, e.g.:

- **GMRT, LOFAR, MWA, LWA, SKA**: interferometric array of radio telescopes at low frequencies ($\nu \simeq (15 - 240)$ MHz)
- **Simbol-X/NuSTAR**: future hard X-ray satellites ($E \simeq (1 - 100)$ keV)
- **Fermi** γ -ray space telescope ($E \simeq (0.1 - 300)$ GeV)
- **Imaging air Čerenkov telescopes** ($E \simeq (0.1 - 100)$ TeV)

Non-thermal emission from clusters

Exploring the memory of structure formation

- **primary, shock-accelerated CR electrons** resemble current accretion and merging shock waves
- **CR protons/hadronically produced CR electrons** trace the time integrated non-equilibrium activities of clusters that is modulated by the recent dynamical activities

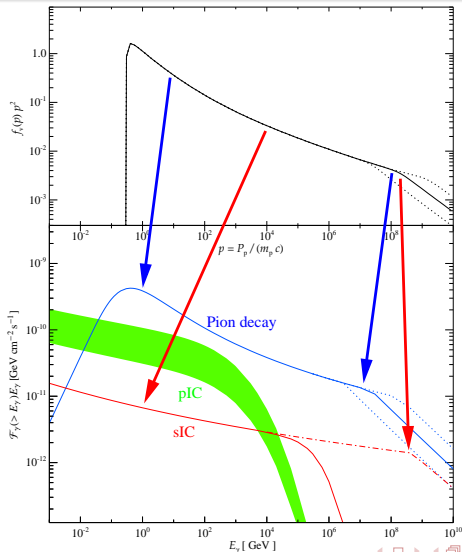
How can we read out this information about non-thermal populations?

→ **new era of multi-frequency experiments**, e.g.:

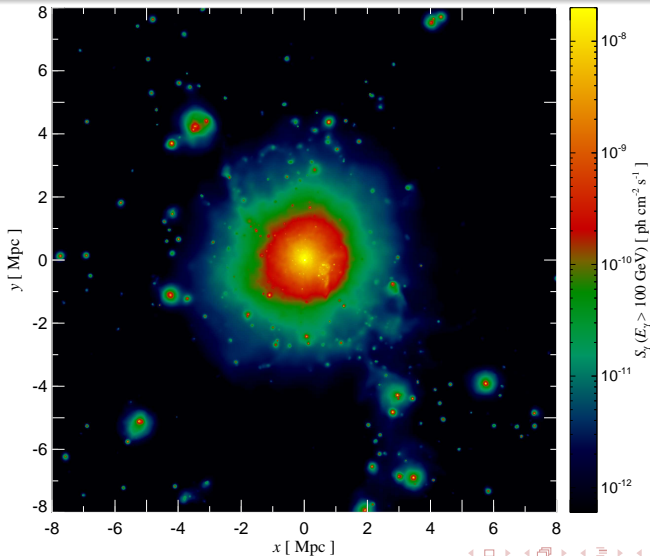
- **GMRT, LOFAR, MWA, LWA, SKA**: interferometric array of radio telescopes at low frequencies ($\nu \simeq (15 - 240)$ MHz)
- **Simbol-X/NuSTAR**: future hard X-ray satellites ($E \simeq (1 - 100)$ keV)
- **Fermi** γ -ray space telescope ($E \simeq (0.1 - 300)$ GeV)
- Imaging air **Čerenkov telescopes** ($E \simeq (0.1 - 100)$ TeV)



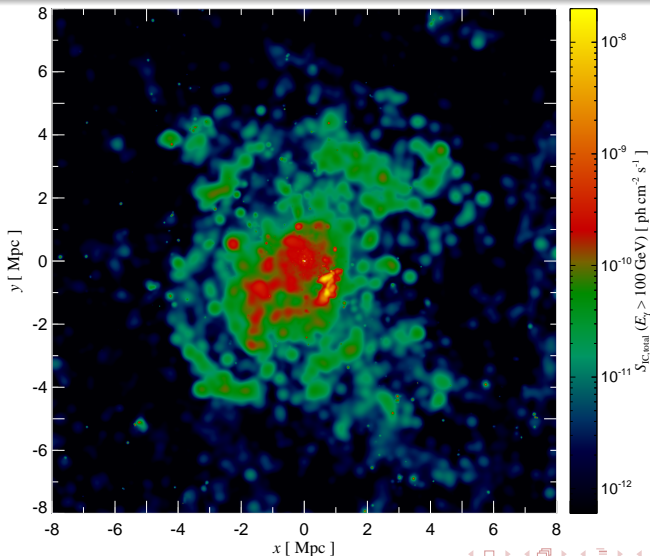
CR proton and γ -ray spectrum (Pinzke & CP 2010)



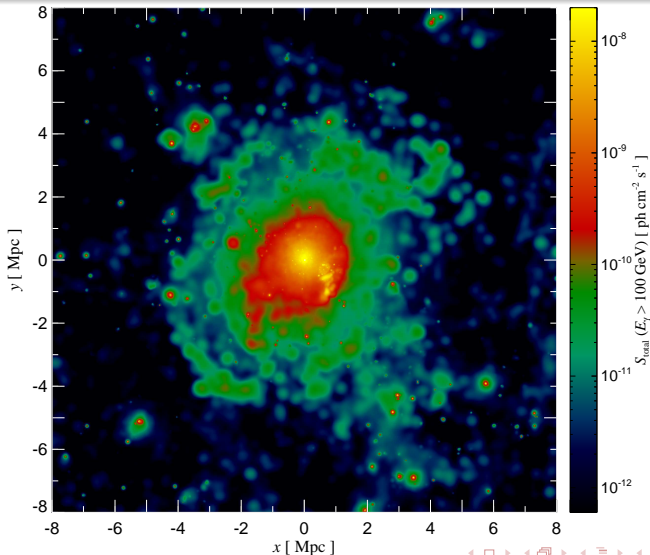
Hadronic γ -ray emission, $E_\gamma > 100$ GeV



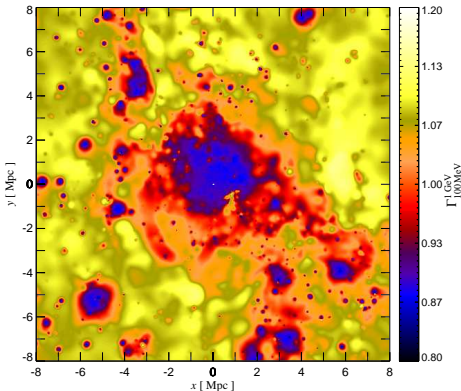
Inverse Compton emission, $E_{IC} > 100$ GeV



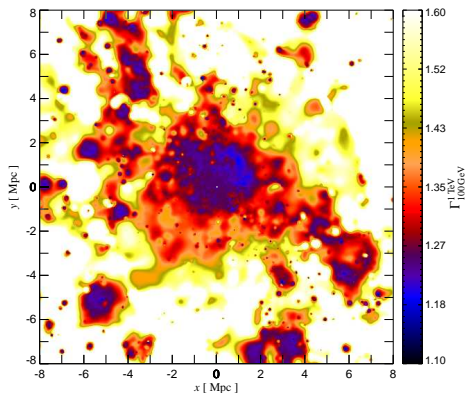
Total γ -ray emission, $E_\gamma > 100$ GeV



Photon index Γ - variations on large scales

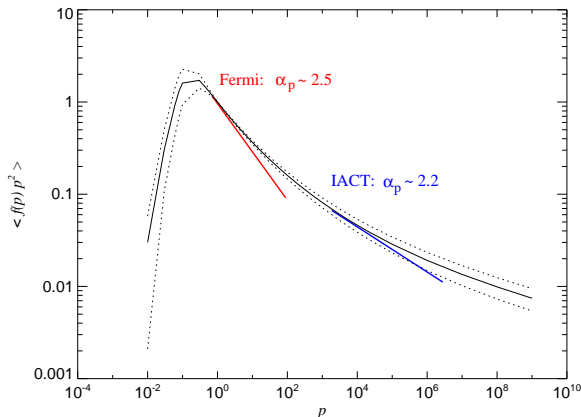


$\Gamma_{100\text{MeV}}^1$ [GeV] (Fermi): pion bump (center)
transition to pIC (strong accretion shocks)



$\Gamma_{100\text{GeV}}^1$ [TeV] (IACT's): pion-decay (center)
pIC (accretion shocks, cutoff E_{max})

Universal CR spectrum in clusters

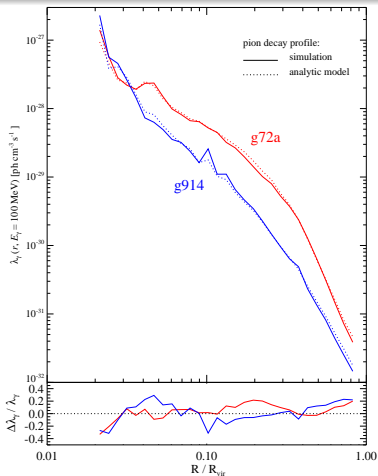


Normalized CR spectrum shows **universal concave shape** \rightarrow governed by hierarchical structure formation and the implied distribution of Mach numbers that a fluid element had to pass through in cosmic history (Pinzke & CP 2010).

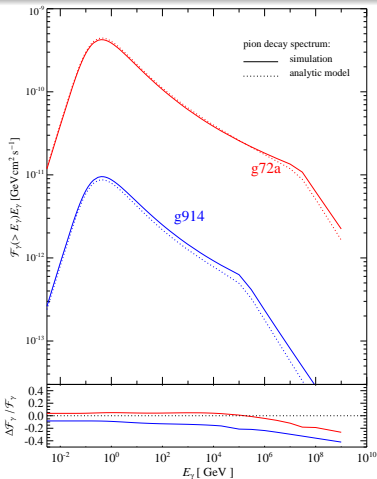


An analytic model for the cluster γ -ray emission

Comparison: simulation vs. analytic model, $M_{\text{vir}} \simeq (10^{14}, 10^{15}) M_{\odot}$

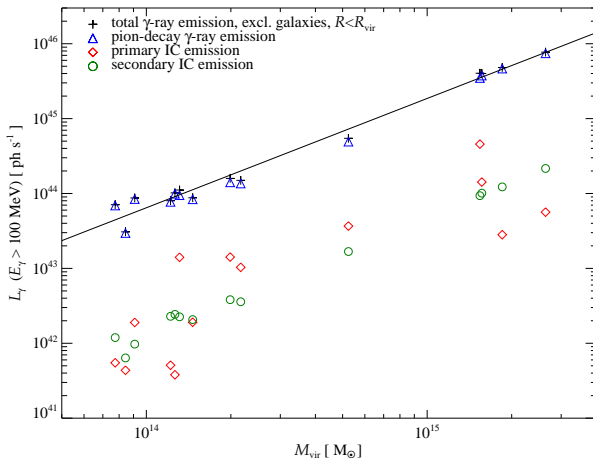


Spatial γ -ray emission profile



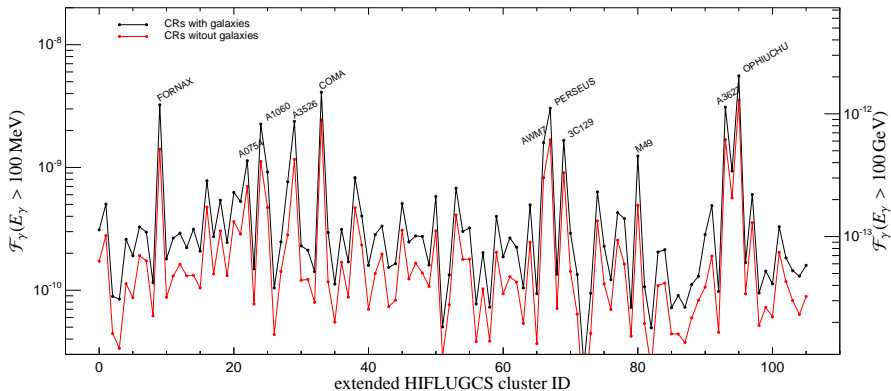
Pion decay spectrum

Gamma-ray scaling relations



Scaling relation + complete sample of the brightest X-ray clusters (HIFLUGCS) \rightarrow predictions for *Fermi* and *IACT*'s

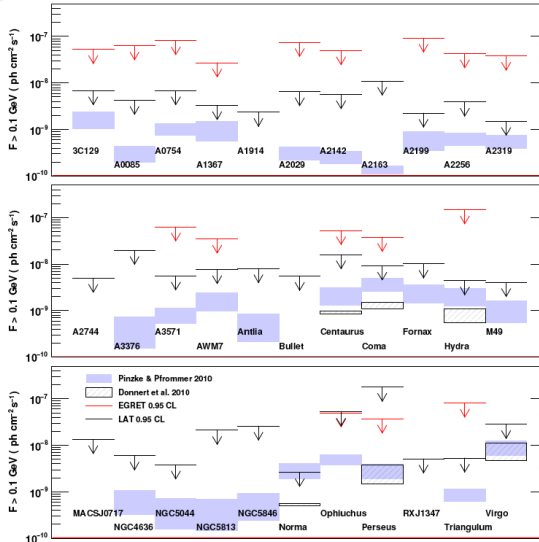
Predicted cluster sample for *Fermi* and *IACT*'s



black: optimistic model, including galactic 'point sources' that bias γ -ray flux high;
 red: realistic model, excluding galactic 'point sources'



γ -ray flux limits from *Fermi* (Ackermann et al. 2010)



Outline

- 1 Magnetic draping on spiral galaxies
 - Polarized radio ridges
 - Physics of magnetic draping
 - Implications and speculations
- 2 Cosmic rays in clusters
 - Physical processes
 - Cosmological simulations
 - Gamma-ray emission
- 3 **Conclusions**



Conclusions

In contrast to the thermal plasma, the non-equilibrium distributions of CRs preserve the information about their injection and transport processes and provide thus a unique window of current and past structure formation processes and diffusive shock acceleration!

Universal distribution of CR protons determined by maximum shock acceleration efficiency ζ_{\max} and adiabatic transport: mapping between the hadronic γ -ray emission and ζ_{\max}

- cosmological simulations are indispensable for exploring this (non-linear) map
- *Fermi* limits are in agreement with simulations using most optimistic assumptions of CR acceleration and transport
- spectral shape illuminates the process of structure formation



Conclusions

In contrast to the thermal plasma, the non-equilibrium distributions of CRs preserve the information about their injection and transport processes and provide thus a unique window of current and past structure formation processes and diffusive shock acceleration!

Universal distribution of CR protons determined by maximum shock acceleration efficiency ζ_{\max} and adiabatic transport: mapping between the hadronic γ -ray emission and ζ_{\max}

- cosmological simulations are indispensable for exploring this (non-linear) map
- *Fermi* limits are in agreement with simulations using most optimistic assumptions of CR acceleration and transport
- spectral shape illuminates the process of structure formation



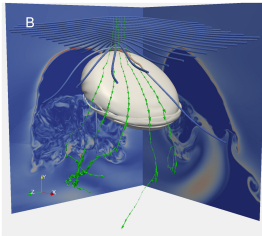
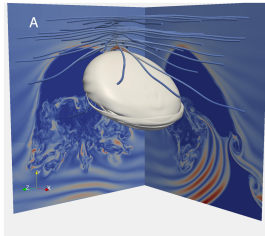
Literature for the talk

- Pfrommer & Dursi, 2010, Nature Phys. 6, 520-526, *Detecting the orientation of magnetic fields in galaxy clusters*
- Pinzke & Pfrommer, 2010, MNRAS, accepted, arXiv:1001.5023, *Simulating the gamma-ray emission from galaxy clusters: a universal cosmic ray spectrum and spatial distribution*
- Pfrommer, 2008, MNRAS, 385, 1242, *Simulating cosmic rays in clusters of galaxies – III. Non-thermal scaling relations and comparison to observations*
- Pfrommer, Enßlin, Springel, 2008, MNRAS, 385, 1211, *Simulating cosmic rays in clusters of galaxies – II. A unified scheme for radio halos and relics with predictions of the γ -ray emission*
- Pfrommer, Enßlin, Springel, Jubelgas, Dolag, 2007, MNRAS, 378, 385, *Simulating cosmic rays in clusters of galaxies – I. Effects on the Sunyaev-Zel'dovich effect and the X-ray emission*
- Enßlin, Pfrommer, Springel, Jubelgas, 2007, A&A, 473, 41, *Cosmic ray physics in calculations of cosmological structure formation*

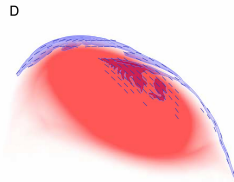


Magnetic draping of a non-uniform B-field

(Non-)observation of polarization twist constrains magnetic coherence length



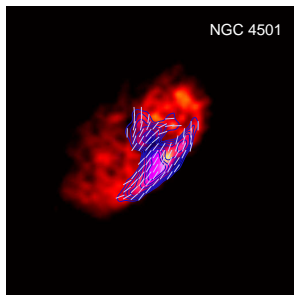
Total PI = 1.586 mJ
Max PI = 67.42 μ J/beam



Total PI = 5.927 mJ
Max PI = 304.9 μ J/beam



Magnetic coherence scale estimate by radio ridges



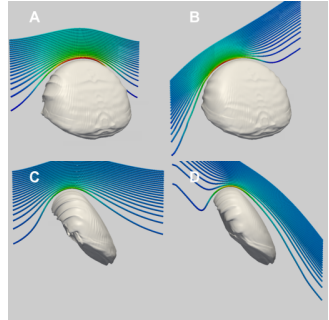
- observed polarised draping emission
→ field coherence length λ_B is at least galaxy-sized
- if $\lambda_B \sim 2R_{\text{gal}}$, then the change of orientation of field vectors imprint as a change of the polarisation vectors along the vertical direction of the ridge showing a ‘polarisation-twist’
- the reduced speed of the boundary flow means that a small L_{drape} corresponds to a larger length scale of the unperturbed magnetic field ahead of the galaxy NGC 4501

$$L_{\text{coh}} \simeq \eta L_{\text{drape}} v_{\text{gal}} / v_{\text{drape}} = \eta \tau_{\text{syn}} v_{\text{gal}} > 100 \text{ kpc},$$

with $\tau_{\text{syn}} \simeq 5 \times 10^7 \text{ yr}$, $v_{\text{gal}} \simeq 1000 \text{ km/s}$, and a geometric factor $\eta \simeq 2$

Biases in inferring the field orientation

- uncertainties in estimating the 3D velocity: v_r , ram-pressure stripped gas visible in HI morphology $\rightarrow \hat{\mathbf{v}}_t$
- *direction-of-motion asymmetry*: magnetic field components in the direction of motion bias the location of $B_{\max, \text{drape}}$ (figure to the right): draping is absent if $\mathbf{B} \parallel \mathbf{v}_{\text{gal}}$



- *geometric bias*: polarized synchrotron emission only sensitive to traverse magnetic field B_t (\perp to LOS) \rightarrow maximum polarised intensity may bias the location of $B_{\max, \text{drape}}$ towards the location in the drape with large B_t